Evaluating possible maternal effect lethality of *Naa10* knockout mice, and modulation of phenotypes for embryonic and neonatal lethality by genetic background and environment

Gholson J. Lyon[1,2*], Joseph Longo[1,#], Andrew Garcia[1,2,#], Fatima Inusa[1], Elaine Marchi[1], Daniel Shi[1], Max Dörfel[3,4], Thomas Arnesen[5,6,7], Rafael Aldabe[8], Scott Lyons[3], Melissa Nashat[1], David Bolton[9]

[1]Human Genetics Department, New York State Institute for Basic Research (IBR) in Developmental Disabilities, Staten Island, New York, USA

[2]Biology PhD Program, The Graduate Center, The City University of New York, New York, USA

[3]Stanley Institute for Cognitive Genomics, Cold Spring Harbor Laboratory, Woodbury, New York, USA

[4]Bausch + Lomb, Dr. Gerhard Mann Chem.-Pharm. Fabrik GmbH, Berlin, Germany

[5]Department of Biomedicine, University of Bergen, Bergen, Norway

[6]Department of Biological Sciences, University of Bergen, Bergen, Norway

[7]Department of Surgery, Haukeland University Hospital, Bergen, Norway

[8]Division of Gene Therapy and Regulation of Gene Expression, CIMA, University of Navarra, Pamplona, Spain

[9]Molecular Biology Department, New York State Institute for Basic Research (IBR) in Developmental Disabilities, Staten Island, New York, USA

#co-second authors

* Corresponding author

gholsonjlyon@gmail.com / gholson.j.lyon@opwdd.ny.gov (GJL)

ABSTRACT

Amino-terminal (Nt-) acetylation (NTA) is a common protein modification, affecting approximately 80% of all human proteins. The human essential X-linked gene, *NAA10,* encodes for the enzyme NAA10, which is the catalytic subunit in the N-terminal acetyltransferase A (NatA) complex, also including the accessory protein, NAA15, encoded by the autosomal gene, *NAA15*. Although *NAA10* is an essential gene in humans, there is nonetheless extensive genetic variation in humans with missense, splice-site, and C-terminal frameshift variants in *NAA10*. Likewise, the genetic spectrum for *NAA15 is* also extensive, where the mechanism likely involves haploinsufficiency in heterozygous individuals. The phenotypic presentation in humans with *NAA10* or *NAA15* variants includes variable levels of intellectual disability, delayed milestones, autism spectrum disorder, craniofacial dysmorphology, cardiac anomalies, seizures, and visual abnormalities. In mice, *Naa10* is not an essential gene, as there exists a paralogous gene, *Naa12*, that substantially rescues *Naa10* knockout mice from embryonic lethality, whereas double knockouts ($Naa10^{-/Y}$ Naa12$^{-/-}$) are embryonic lethal. However, the phenotypic variability in the mice is nonetheless quite extensive, including piebaldism, skeletal defects, small size, hydrocephaly, hydronephrosis, and neonatal lethality. Here we show that the mouse phenotypes are replicated with new genetic alleles, but are modulated by genetic background and environmental effects, as demonstrated by several new mouse strains and backcrossing of the original *Naa10* null allele 20 generations to inbred C57BL/6J mice in a different animal facility. We cannot replicate a prior report of "maternal effect lethality" for heterozygous $Naa10^{-/X}$ female mice, but we do observe a small amount of embryonic lethality in the $Naa10^{-/y}$ male mice on the inbred genetic background in this different animal facility. We hypothesize that decreased NTA of many different target substrate proteins is the main explanation for the variable phenotypic outcomes, and future experiments will make use of these mice and human cell lines to address this hypothesis.

INTRODUCTION

Targeting 40% of the human proteome, NatA, the major N-terminal acetyltransferase (NAT) complex, acetylates Ser-, Ala-, Gly-, Thr-, Val-, and Cys- N-termini following cleavage of the initiator methionine (Thomas Arnesen et al. 2009; Starheim, Gevaert, and Arnesen 2012). The canonical human NatA consists of two main subunits, the catalytic subunit N-α-acetyltransferase 10 (*NAA10*) (Ard1) and the auxiliary subunit NAA15 (Nat1) and engages with a regulatory subunit, HYPK (Thomas Arnesen et al. 2005, 2010; Gottlieb and Marmorstein 2018). N-terminal (Nt-) acetylation (NTA) is one of the most common protein modifications, occurring co- and post-translationally (M. J. Dörfel and Lyon 2015; Aksnes, Ree, and Arnesen 2019). Approximately 80% of cytosolic proteins are N-terminally acetylated in humans and ~50% in yeast (Thomas Arnesen et al. 2009), while NTA is less common in prokaryotes and archaea (M. J. Dörfel and Lyon 2015).

NTA is catalyzed by a set of enzymes, the NATs, which transfer an acetyl group from acetyl coenzyme A (Ac-CoA) to the free α-amino group of a protein's N-terminus. To date, eight distinct NATs (NatA – NatH) have been identified in metazoan (NatA-F and NatH) and plant (NatG) species that are classified based on different conserved subunit compositions and substrate specificities (B. Polevoda, Arnesen, and Sherman 2009; Aksnes, Ree, and Arnesen 2019; Starheim, Gevaert, and Arnesen 2012). NTA has been implicated in steering protein folding, stability or degradation, subcellular targeting, and complex formation (R. Ree, Varland, and Arnesen 2018; Shemorry, Hwang, and Varshavsky 2013; Dikiy and Eliezer 2014; Scott et al. 2011; Holmes et al. 2014). Particularly, Naa10-catalyzed N-terminal acetylation has been reported to be essential for development in many species (Y. Wang et al. 2011; D. Chen et al. 2014; Linster et al. 2015; Feng et al. 2016; H. Chen et al. 2018) and although NatA is not essential in *S. cerevisiae*, depletion of *Naa10* or Naa15 has strong effects, including slow growth and decreased survival when exposed to various stresses (Mullen et al. 1989; Bogdan Polevoda and Sherman 2003). In addition, it has been recently shown that mice have a compensating enzyme Naa12, which prevents embryonic lethality in the *Naa10* knockouts (Kweon et al. 2021), but a

similar gene has not been found in humans. Furthermore, given that *NAA10* was also identified in screens for essential genes in human cell lines (Blomen et al. 2015; T. Wang et al. 2015), it seems unlikely that an unknown *NAA10*-like paralogous gene exists in humans, other than the already known *NAA11* (Pang et al. 2011; T. Arnesen et al. 2006).

Ogden syndrome (OS), was first reported and named in 2011 after the location of the first affected family residing in Ogden, Utah, USA (Rope et al. 2011; G. J. Lyon 2011). In that first family, five males were born to four different mothers and all the males died in early infancy, with a range of cardiac, phenotypic variation and other defects, including lethal cardiac arrhythmias. The underlying genetic defect was characterized as a single missense change coding for Ser37Pro in the X-linked gene, *NAA10*, and was confirmed in a second independent family in California, USA, with three males that also died during infancy. The identical variant was recently reported in a third family (Gogoll et al. 2021), and a fourth family (Hofman et al. 2022). There is a *S. cerevisiae* model for the *Naa10* Ser37Pro mutant, in which that variant impairs NatA complex formation and leads to a reduction in both NatA catalytic activity and functionality (Van Damme et al. 2014; Max J. Dörfel et al. 2017). Furthermore, OS patient-derived cells have impaired *in vivo* NTA of a few NatA substrates (Myklebust et al. 2015).

Since the initial discovery of OS in 2011, multiple groups have reported additional variants either in *NAA10* in both males and females (Bader et al. 2020; Casey et al. 2015; Hanyin Cheng et al. 2019; McTiernan et al. 2021; Popp et al. 2015; Rasmus Ree et al. 2019; Støve et al. 2018; Afrin et al. 2020; Esmailpour et al. 2014; Johnston et al. 2019; Gupta et al. 2019; Saunier et al. 2016; Maini et al. 2021; McTiernan et al. 2022) or in the heterodimeric protein partner encoded by *NAA15* (Cheng et al. 2019; Cheng et al. 2018; Ritter et al. 2021; Ward et al. 2021; Tian et al. 2022). The genetic landscape of variation in *NAA10* and *NAA15* in humans has been presented recently with many more cases of Ogden syndrome (OS) (also known as "*NAA10*-related neurodevelopmental syndrome"), and "*NAA15*-related neurodevelopmental syndrome" (Lyon et al. 2022).

Previous publications have reported that one of the phenotypes observed in *Naa10* knockout mice is low body weight compared to their wildtype littermates (Kweon et al. 2021; Lee et al. 2017). A recent analysis in humans analyzed these growth defects in greater detail, which showed extensive weight fluctuations, along with the recommendation that OS individuals not tracking above the failure to thrive range past one year of age might be considered for G-tube placement to avoid prolonged growth failure (Sandomirsky et al. 2023). The current study aims to characterize the development, growth and phenotypes of various mice deficient in *Naa10*, beginning with embryogenesis, thus extending and expanding on our prior findings (Kweon et al. 2021).

RESULTS

Independently generated knockdown (KD) and knockout mice for *Naa10* demonstrate similar phenotypes.

Twice we attempted to develop a mouse model for Ogden Syndrome with a Ser37Pro missense mutation found in the first family identified with this syndrome (Rope et al. 2011). The first attempt included the use of a minigene for exons 2-3, which was inserted in an intron in *Naa10*, that could theoretically then be activated upon inversion of the cassette by crossing to Cre-expressing animals (see **Supplementary Figure 1** for gene targeting design). Unfortunately, both Western blotting and quantitative PCR revealed that the insertion of this minigene in the intron between exons 3 and 4, regardless of its inversion status, led to >95% knockdown of expression of *Naa10* (**Supplementary Figure 2** and **3**). As such, the interpretation of any results in this mouse model for the Ogden Syndrome Ser37Pro mutation are complicated by the knockdown of *Naa10*. We refer to these mice as male $Naa10^{mini/Y}$, female $Naa10^{mini/mini}$, male $Naa10^{invS37P/Y}$, and female $Naa10^{invS37P/invS37P}$. When tabulating the Mendelian ratios, with genotyping performed after weaning around four weeks of age, there was a slight deviation (22%) from the predicted Mendelian ratio (25%) for the male $Naa10^{mini/Y}$ mice (**Supplementary Table 1**)

and a much larger deviation (13%) for the male $Naa10^{invS37P/Y}$ mice (**Supplementary Table 2**), which suggests the possibility that the S37P mutation does indeed exert a hypomorphic effect on NatA function. However, the confound for any interpretation of these data is the presence of severe knockdown of overall $Naa10$ protein expression, given that the minigene apparently has some effect on RNA expression or stability (**Supplementary Figure 2B**).

The phenotypes of these Naa10 knockout mice are similar to previously published identifying characteristics including piebaldism, hydrocephaly, cardiac defects, homeotic anterior transformation, and urogenital anomalies (Kweon et al. 2021). Although there was complete penetrance for piebaldism in the male mice, there was variable amounts of this, which was quantified to show the high variability of this phenotype in this allelic series of mutant mice (**Supplementary Figure 4**). Piebaldism was also present and quantified in female $Naa10^{mini/mini}$ and female $Naa10^{invS37P/\ invS37P}$ mice, with no obvious correlation between the amount of piebaldism and the genotype, age, or weight of the mice (**Supplementary Figure 5**). Piebaldism in heterozygous females was only very rarely seen (on the order of 1-2 animals among >40 animals per allele). Another phenotype identified with complete penetrance was bilateral supernumerary ribs (14 pairs of rib instead of 13) in all male $Naa10^{mini/Y}$, female $Naa10^{mini/mini}$, male $Naa10^{invS37P/Y}$, and female $Naa10^{invS37P/\ invS37P}$ (**Supplementary Table 3**). This extra pair of ribs linking to the sternum transforms the T8 vertebrae into an anterior T7-like phenotype. Many of these mice also had four instead of the usual three sternebrae, which were sometimes fused. Cervical vertebrae fusion was also demonstrated in these mice, particularly involving C1 and C2, suggesting possible anteriorization of C2 into a C1-like phenotype (**Supplementary Table 4**). These phenotypes are identical to what was described in the $Naa10^{-/y}$ mice (Kweon et al. 2021).

Bone density of calvarias was measured using computerized tomography (CT) scanning (**Supplementary Figure 6**), showing no difference from wild type, except in a few of the $Naa10^{-/y}$ mice where hydrocephaly developed, accompanied by dilatation of the skull over time with thinning of the calvarium. As such, the published calvarial bone density phenotype reported in

three day old *Naa10*^{-/Y} mice (Yoon et al. 2014) does not remain by adulthood. Femur bone density did show a small but statistically significant decrease in the male *Naa10*^{-/y} mice and *Naa10*^{invS37P/y} mice, compared to the *Naa10*^{+/y} and *Naa10*^{mini/y} mice (**Supplementary Figure 7B**), and the female heterozygous *Naa10*^{+/invS37P} also had slightly decreased femur bone density compared to *Naa10*^{+/+} and *Naa10*^{+/-} mice (**Supplementary Figure 7D**). However, these data are limited by the fact that these measurements were taken in mice at all ages, and the overall number of mice was small in some groups (e.g., n=3 for *Naa10*^{+/invS37P}) (**Supplementary Figure 7A** and **7C**). Furthermore, the *Naa10*^{-/Y} mice were still on a somewhat mixed genetic background at the time of these experiments, as the number of backcrosses to C57BL/6J had only reached about 12-13 backcrosses at that time. Future experiments should ideally repeat this with a larger number of mice at one age timepoint, ideally on an inbred C57BL/6J genetic background (>20 backcrosses or mice generated at the outset from zygotes from an inbred background).

The second attempt to generate *Naa10*^{S37P/y} mice included four rounds of microinjection (see **Supplementary Table 5**) of CRISPR reagent mix including guide RNA and oligonucleotide donor into zygotes obtained from the mating of B6D2F1 females (i.e. 50% C57BL/6J, 50% DBA/2J (D2)) females to inbred C57BL/6J males (Jackson Laboratories, Bar Harbour, ME, USA). The guide RNA was produced and validated from Horizon (Perkin Elmer, USA), using a Cel1-nuclease assay, and the most active guide was selected, including the targeting cr-RNA sequence and the tracrRNA portion. Despite screening 156 offspring from these four injections, only indels were obtained, with no evidence of homologous recombination with the oligonucleotide donor to generate the desired Ser37Pro missense mutation. Two of the indels, namely a one base pair deletion (Δ668) and a seven base pair deletion (Δ668-674) were successfully transmitted to the next generation by backcrossing to C57BL/6J mice. Western blotting and qPCR confirmed knockout of *Naa10* due to the frameshifts introduced by the indels (**Supplementary Figure 8**). Breeding of these mice on this mixed genetic background did not show any obvious embryonic or neonatal lethality for the Δ668 male mice or the Δ668-674 male mice, as they were born and

genotyped in the first week of life with no deviation from the expected 25% Mendelian ratios (**Supplementary Table 6** and **7**). Although most of these knockout mice had piebaldism, some of them did not (6 out of 81 Δ668 male mice and 10 out of 36 Δ668-674 male mice without piebaldism). The *Naa10* indel mice also have bilateral supernumerary ribs (14 pairs of rib instead of 13), and a majority of these mice also had four instead of the usual three sternebrae, which were sometimes fused (**Supplementary Table 3**), as previously reported (Kweon et al. 2021). Cervical vertebrae fusion was also demonstrated in these mice (**Supplementary Table 4**). Out of all mice that were generated in the above and other matings, hydrocephaly did develop in the *Naa10* Δ668 male mice (23/62, or 37%) and in the *Naa10* Δ668-674 male mice (16/45, or 36%), which is similar to the previously reported rate around 40% (Kweon et al. 2021) and substantially higher than the rate of 1% in wild type mice on the C57BL/6J genetic background.

As these new strains of knockdown or knockout mice recapitulated the phenotype of the already established *Naa10* knockout (KO) lines (Kweon et al. 2021), it was decided to not maintain these lines, so the minigene and indel strains were euthanized, with sperm cryopreservation at Cold Spring Harbor Laboratory (CSHL), available upon request.

Validation of a specific *Naa10* antibody and demonstration of heterozygous expression in female *Naa10* mice
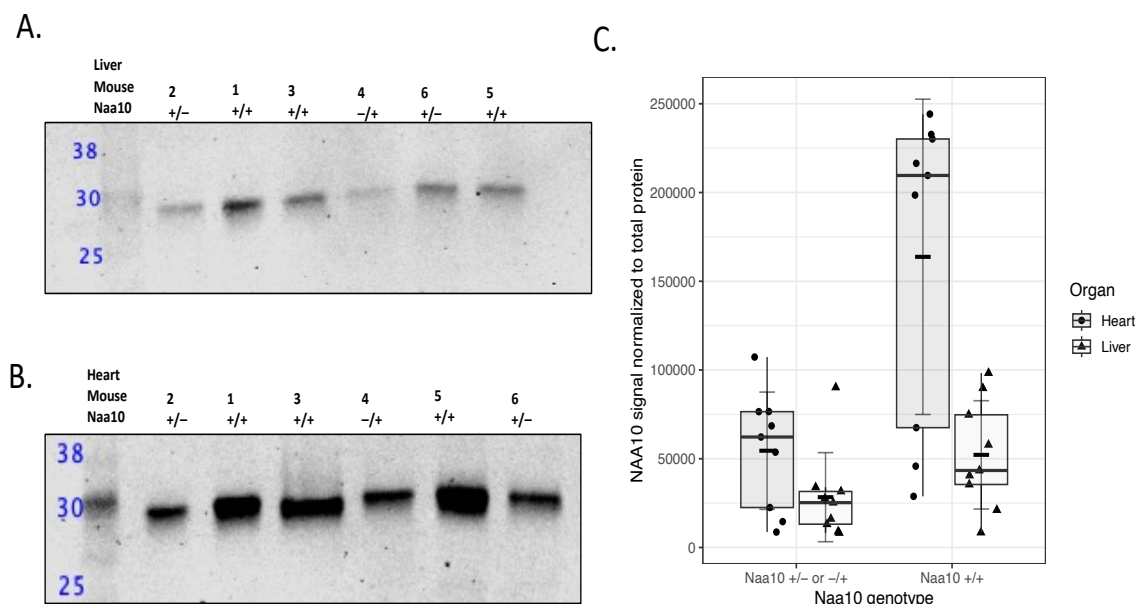
Prior Western blotting using the *Naa10* antibody obtained from Abcam always demonstrated a cross-reactive band of the same molecular weight as *Naa10*, which can be seen in the Western blot data in **Supplementary Figure 2** and **3**. We hypothesized that this cross-reactive band might be the recently discovered mouse Naa12 (Kweon et al. 2021). A new rabbit monoclonal anti-*Naa10* antibody is now available from Cell Signaling Technologies, Danvers, MA, USA, #13357, and this antibody was made with synthetic peptide corresponding to residues surrounding Asp204 of human NAA10. This is a region that diverges from mouse Naa12 (Kweon et al. 2021), so there should not be any cross-reactivity to Naa12. This was confirmed by Western

blotting from tissues isolated from male mice. Biological replicates (n = 8) were obtained consisting of $Naa10^{-/Y}$ (n = 4) and $Naa10^{+/Y}$ (n = 4) animals **(Supplementary Figure 9)**. Per genotype, the mean $Naa10$ signal normalized to total protein detected in $Naa10^{-/Y}$ was <10% of the $Naa10^{+/Y}$ animals, a significant difference between genotypes (2-way ANOVA, F statistic = 14.52 on 3 and 12 DF, p < 0.05).

Using this $Naa10$-specific antibody, we quantified the relative amounts of $Naa10$ in heterozygous female mice (**Supplementary Figure 10** and **11**). For quantification, Naa10 signal was normalized to total protein in each lane of a gel; post-transfer membranes were stained for total protein and scanned to verify transfer and equal loading before proceeding with Naa10 immunostaining. Liver and heart tissue lysates were prepared from $Naa10^{-/+}$ and/or $Naa10^{+/-}$ (n = 3) and $Naa10^{+/+}$ (n = 3) mice obtained from our animal colony. The former heterozygous genotypes differ based on the $Naa10$ knockout allele's parent-of-origin. Based on the lack of maternal or paternal effect lethality in the embryonic and postnatal data (discussed below), we grouped the two $Naa10$ heterozygous mutant genotypes together. Western blots using samples from these were repeated in triplicate. Replicate analysis indicates the mean normalized Naa10 signal in $Naa10^{+/-}$ or $Naa10^{-/+}$ animals is approximately 38% that of $Naa10^{+/+}$ animals, a statistically significant difference (2-way ANOVA, F-statistic = 12.52 on 3 and 32 DF, p < 0.05, R-Studio, Boston, MS, USA). According to *post hoc* Tukey testing, the main source of variation in mean NAA10 signal is attributable to genotype differences; organ type is not a significant source of variation, though it participates in a significant interaction with genotype. Notably, the reduction in normalized $Naa10$ signal was more variable compared to the $Naa10^{-/Y}$ dataset. However, for the $Naa10^{-/Y}$ dataset, one biological replicate was examined once in each organ, whereas each organ sample in the heterozygous mutant dataset was replicated three times. An earlier experiment **(Supplementary Figure 11)** used liver lysates from a separate set of mice (n = 6) composed of $Naa10^{-/+}$ (n = 3) and C57 females (n = 3); the mutant line (Yoon et al. 2014) is now genetically inbred, with over 20 backcrosses to C57BL/6J. Compared to wild-type liver lysate, $Naa10$ levels

are substantially reduced (>50%) in heterozygous liver, though this is a non-significant result due

to variability (Welch's 2-sample t-test, t = -1.6784, df = 9.1762, p = 0.1252). Heterozygous female

mice can undergo random X-chromosome inactivation, which can lead to Naa10 variability within
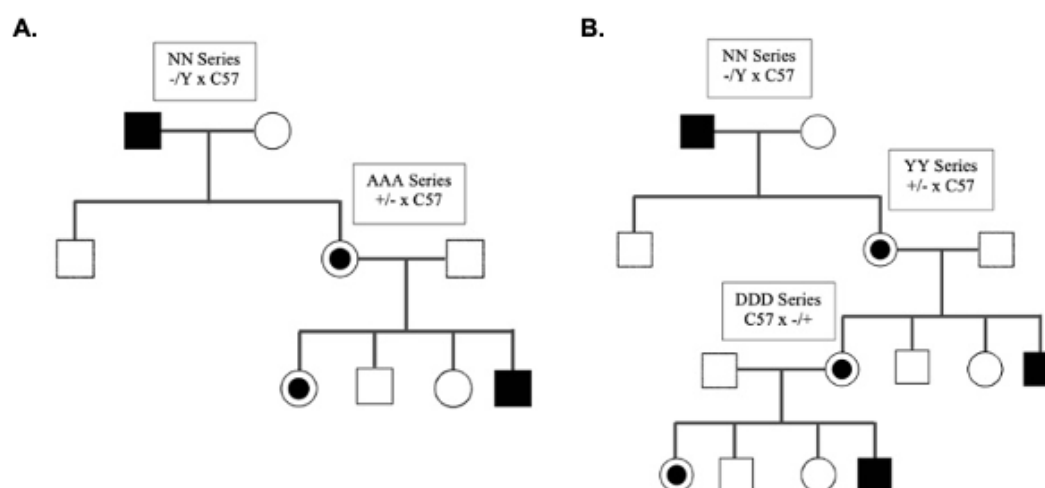
and between tissues.

Figure 1. Western blot analysis of liver and heart lysates from *Naa10* heterozygous mutant female mice. Biological replicates (n = 6) were obtained from *Naa10⁺/⁻* or *Naa10⁻/⁺* mice (N = 3) and *Naa10⁺/⁺* mice (N = 3). Liver and heart lysates were obtained from each mouse for immunoblotting; each liver and heart sample was replicated three times. Blots were stained for total protein post-transfer; after total protein stain removal, blots were incubated with anti-NAA10 MAb and anti-rabbit secondary). **A)** Representative western blot of NAA10 in liver lysates. **B)** Representative western blot of NAA10 in heart lysates. **C)** Quantification of NAA10 signal normalized to total protein. Short black crossbar indicates mean NAA10 signal normalized to total protein (±SD, 2-way ANOVA, F-statistic = 12.52 on 3 and 32 DF, $p < 0.05$).

Effects of environment, genetic background, and parent-of-origin

Given our findings related to genetic background on the phenotypes in the mice discussed above, we analyzed the phenotypes of *Naa10* mice after being backcrossed for 20 generations with C57BL/6J mice; however, this analysis was complicated by the change of colony venue in March 2019, when the backcross was at the 15th generation. Once the backcross was completed to 20 generations, the embryonic dissections and live births occurred in this new environment. A

second aspect of the experiment was meant to address whether *Naa10* is associated with "maternal effect lethality", as a different group argued that maternal inheritance of the *Naa10* knockout allele can have an effect with possible embryonic lethality for ~20% of heterozygous Naa10$^{-/X}$ females (Lee et al. 2017). They used a nomenclature where Naa10$^{-/X}$ mice inherit the null allele maternally, whereas *Naa10*$^{X/-}$ female mice inherit the null allele paternally. We will use Naa10$^{-/X}$ and Naa10$^{-/+}$ interchangeably in the remainder of this manuscript. We have previously presented data that minimizes this effect and suggested lethality might be due to other unidentified factors, such as decreased maternal care of offspring (Kweon et al. 2021). To address this further, several new breedings were undertaken, as detailed in **Figure 2A** and **2B.** For example, embryos with maternal grandfather inherited *Naa10* knockout are designated as the AAA mating series, whereas embryos with maternal grandmother inherited *Naa10* knockout alleles are designated as the DDD mating series (with these letter combinations assigned based on internal lab databases).

Figure 2. Matings used to generate offspring and embryos. The *Naa10* knockout allele is inherited paternally in the NN series, whereas it is inherited maternally in the YY series. For embryo dissections AAA and DDD series, the allele is maternally inherited for both, but the origin of the allele is from the grandfather for the embryos from the AAA series and from the grandmother for the embryos in the DDD series. These letter combinations (like NN, YY, AAA, DDD) are arbitrary and assigned based on internal lab databases.

The Mendelian ratios for embryos from the AAA and DDD matings with the predicted genotypes are shown in **Table 1**, along with the data combined together for AAA and DDD matings. The embryonic age ranged from E9.5 to E16.5, with the bulk of these matings falling between E9.5 to E13.5, as confirmed by Theiler staging comparison. There was some small degree of embryonic lethality (~20-25%) for $Naa10^{-/y}$ mice in both mating series, which is different from its absence in a somewhat mixed genetic background of mice bred in an animal facility in Korea, after at least 6 backcrosses to C57BL/6J (Kweon et al. 2021).

Table 1. Genotypes of E9.5-E13.5 embryos from different mating series

$Naa10^{x/-}$ female mice crossed to $C57BL/6J$ male mice (AAA series)

Genotype (Expected Mendelian %)	$Naa10^{+/y}$ (25%)	$Naa10^{-/y}$ (25%)	$Naa10^{+/+}$ (25%)	$Naa10^{-/+}$ (25%)	Unable to genotype	Resorptions
Embryos + resorptions (n=98)	19 (19.6%)	16 (16.5%)	24 (24.7%)	28 (28.6%)	1 (1.0%)	10 (10.3%)

$Naa10^{-/x}$ female mice crossed to $C57BL/6J$ male mice (DDD series)

Genotype (Expected Mendelian %)	$Naa10^{+/y}$ (25%)	$Naa10^{-/y}$ (25%)	$Naa10^{+/+}$ (25%)	$Naa10^{-/+}$ (25%)	Unable to genotype	Resorptions
Embryos + resorptions (n=75)	21 (28.00%)	13 (17.33%)	17 (22.67%)	17 (22.67%)	0 (0%)	7 (10.29%)

Heterozygous $Naa10^{x/-}$ or $Naa10^{-/x}$ female mice crossed to $C57BL/6J$ male mice (AAA + DDD series)

Genotype (Expected Mendelian %)	$Naa10^{+/y}$ (25%)	$Naa10^{-/y}$ (25%)	$Naa10^{+/+}$ (25%)	$Naa10^{-/+}$ (25%)	Unable to genotype	Resorptions
Embryos + resorptions (n=173)	40 (23.3%)	29 (16.9%)	41 (23.8%)	45 (26.2%)	1 (0.58%)	17 (11.0%)

*Expected and observed Mendelian ratio of genotypes in offspring from crosses, with paw tattoos and tails taken around day 6 of life.

We next examined possible maternal effect lethality. The *Naa10* allele of our AAA mating series is maternally inherited, with the mother of the dissected embryos having inherited the allele from her father (i.e., the maternal grandfather of the AAA embryos), as displayed in the breeding scheme**.** The number of our AAA embryos+resorptions (n=98) versus (n=16) is much larger than in the prior study (Lee et al. 2017) (**Table 1**). There is no statistically significant maternal effect lethality for the heterozygous *Naa10$^{-/X}$* female mice (**Table 2**). **Figure 3a** shows weight gain of dams measured before their mating to their respective sire until the day of necropsy when embryos were harvested, dissected, and measured. *t*-tests comparing the weight gains of C57BL/6J and AAA dams at each length of pregnancy showed no significant statistical difference. **Figures 3B** and **3C** show there is no statistically significant difference in either area or weight of wildtype embryos as compared to *Naa10* knockout embryos in both males and females. Given the larger number of available embryos, within-litter analysis for E12.5 embryos was conducted, and **Figures 4A** and **4B** show four litters only containing E12.5 embryos. The wildtype embryos were greater in area than the knockout mice; however, *t*-tests prove there was no statistical difference between the embryo areas and weights of the wildtype versus knockout embryos. Representative images of the embryos are shown in **Figure 4C**.

The *Naa10* allele in our DDD mating series is also inherited maternally, but with the mother of these embryos having inherited the allele from her mother, i.e., originating from the maternal grandmother. There is no maternal effect lethality for the heterozygous *Naa10$^{-/X}$* female mice (**Table 1** and **Table 2**). **Figure 5A** shows the weight gain of DDD dams and weight gain of dams from the C57BL/6J line. The weight gain values are measured starting from mating date and day of dissection. *T*-tests comparing the weight gain of dams at each length of pregnancy showed no statistically significant difference (p>0.05). **Figures 5B** and **5C** compare embryo areas and weights of *Naa10* knockout male and female embryos compared to the area and weight values of wildtype embryos. There was no statistically significant difference (p>0.05). Within litter analyses were performed on our DDD embryos where there was no statistical difference caused

by variation among different litters. **Figure 6A** shows three litters only containing E12.5 embryos. The smallest area was consistently measured in the *Naa10* knockout embryo. **Figure 6B** shows the weights of the embryos in the three litters. In two of the three litters, the smallest weighing embryo was a *Naa10* knockout. **Figure 6C** shows representative images of the DDD embryos.
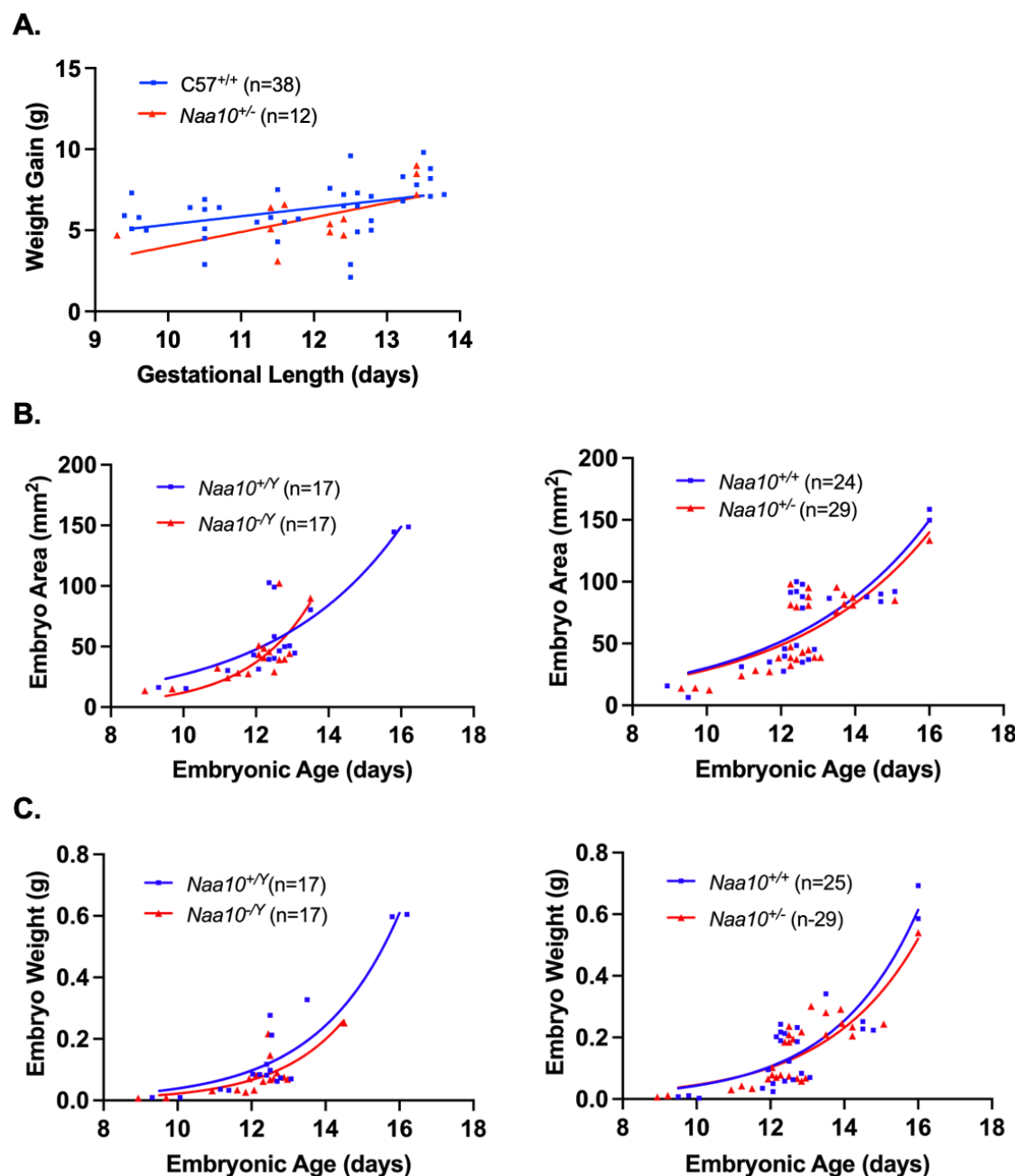
Figure 7A shows no difference in weight gain of the dams' in both the AAA and DDD series matings. The measured embryo areas were not statistically different when analyzed by genotypes. Finally, data of the two breeding groups ranging from E9.5 to E13.5 were combined and shown at the bottom of **Table 1**. The difference in Mendelian ratios based on the number of heterozygous $Naa10^{-/X}$ female mice (n=45) compared to the number of wild type male mice (n=40) is not statistically significant.
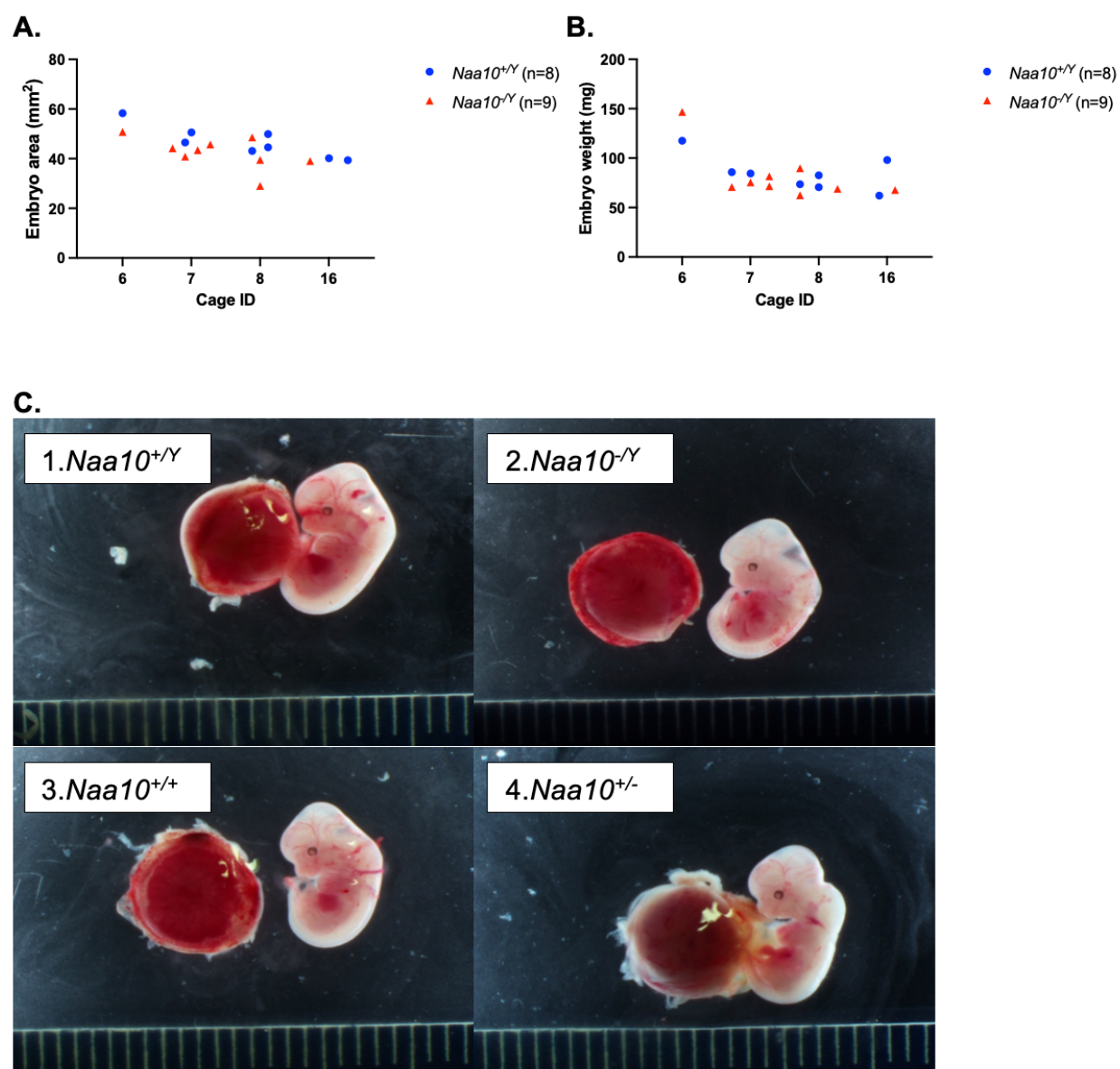
Table 2. Chi Squared Analyses	n-value	Degrees of Freedom	Critical Value	Chi Squared Value	Significant Yes/No
Chi Squared Analysis for all embryonic ages (Analyzing all four genotypes)					
Naa10$^{+/-}$ female mice crossed to C57BL/6J male mice (AAA series)	115	3	7.81	6.89	NO
Naa10$^{-/+}$ female mice crossed to C57BL/6J male mice (DDD series)	108	3	7.81	1.29	NO
Naa10$^{+/-}$ or *Naa10*$^{-/+}$ female mice crossed to C57BL/6J male mice (AAA + DDD series)	223	3	7.81	5.84	NO
Chi Squared Analysis for all embryonic ages (Analyzing only *Naa10*$^{-/Y}$ vs *Naa10*$^{+/-}$and *Naa10*$^{-/+}$)					
Naa10$^{+/-}$ female mice crossed to C57BL/6J male mice (AAA series)	50	1	3.84	5.51	YES
Naa10$^{-/+}$ female mice crossed to C57BL/6J male mice (DDD series)	46	1	3.84	1.25	NO
Naa10$^{+/-}$ or *Naa10*$^{-/+}$ female mice crossed to C57BL/6J male mice (AAA + DDD series)	96	1	3.84	5.18	YES
Chi Squared Analysis for E9.5-E13.5 embryos only (Analyzing all four genotypes)					
Naa10$^{+/-}$ female mice crossed to C57BL/6J male mice (AAA series)	88	3	7.81	2.05	NO
Naa10$^{-/+}$ female mice crossed to C57BL/6J male mice (DDD series)	75	3	7.81	2.78	NO
Naa10$^{+/-}$ or *Naa10*$^{-/+}$ female mice crossed to C57BL/6J male mice (AAA + DDD series)	173	3	7.81	4.95	NO
Chi Squared Analysis for E9.5-E13.5 embryos only (Analyzing only *Naa10*$^{-/Y}$ vs *Naa10*$^{+/-}$and *Naa10*$^{-/+}$)					
Naa10$^{+/-}$ female mice crossed to C57BL/6J male mice (AAA series)	44	1	3.84	3.28	NO
Naa10$^{-/+}$ female mice crossed to C57BL/6J male mice (DDD series)	30	1	3.84	2.1	NO
Naa10$^{+/-}$ or *Naa10*$^{-/+}$ female mice crossed to C57BL/6J male mice (AAA + DDD series)	74	1	3.84	4.65	YES

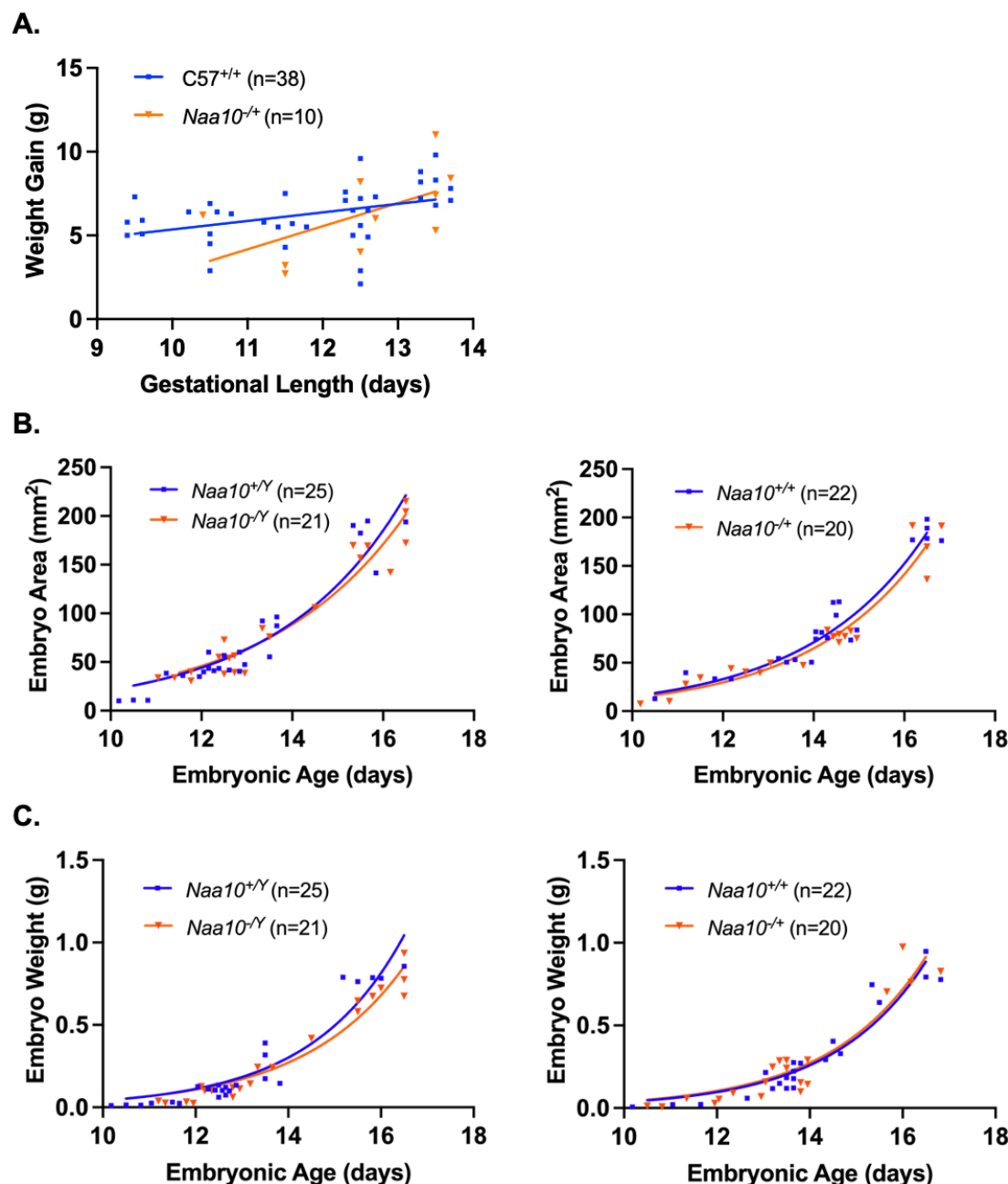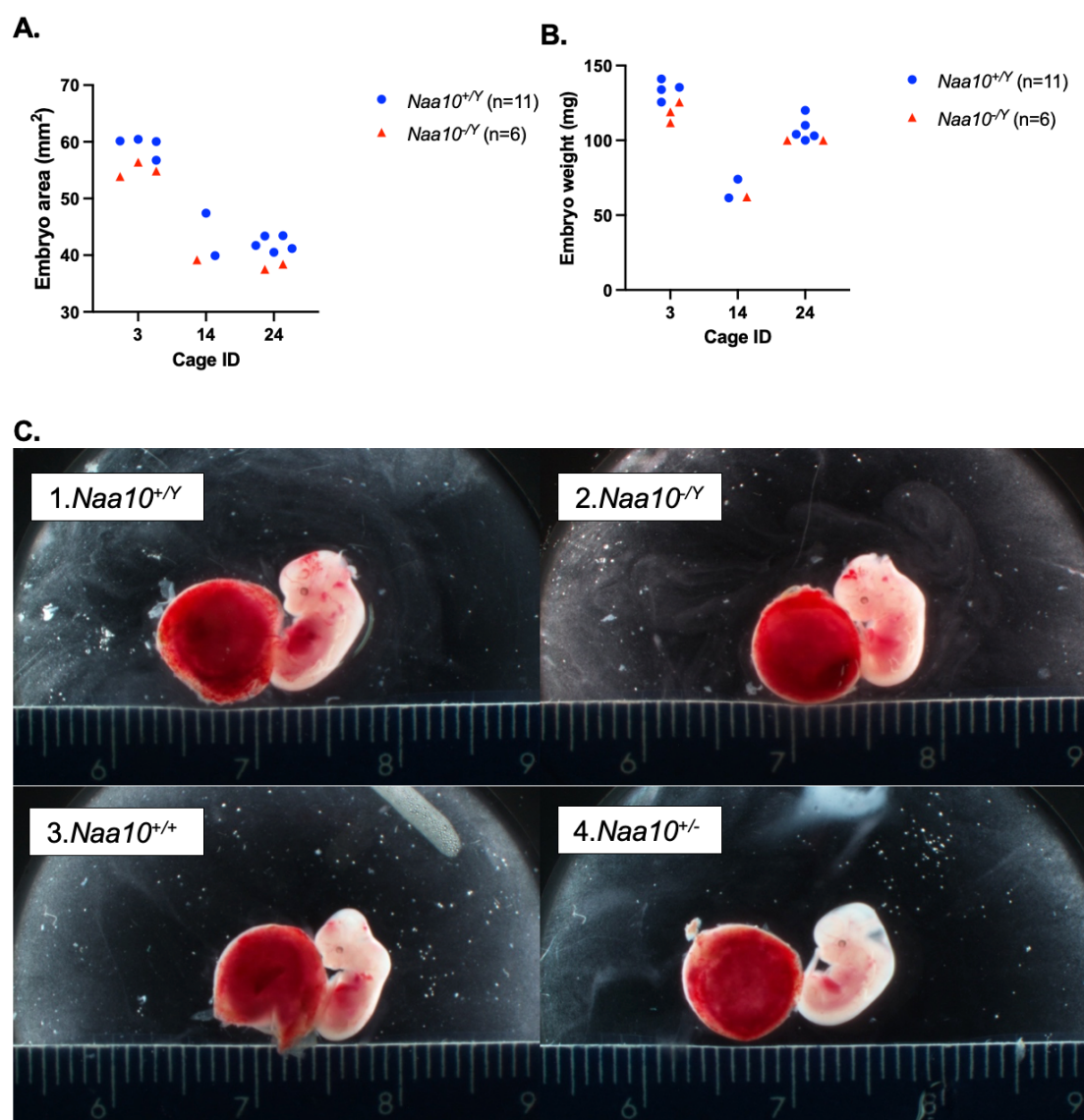*Chi squared analyses calculated using critical value and p-value = 0.05.

Figure 3. Embryonic phenotypes of *Naa10* knockout mice after 20 backcrosses, maternally inherited but originating from the maternal grandfather, and represented here as AAA. **(A)** *Naa10*$^{+/-}$ and *Naa10*$^{+/+}$ dams were weighed and compared at various lengths of gestation. However, there was no statistically significant difference between both simple linear regression lines that represent the weight gains of *Naa10*$^{+/-}$ and *Naa10*$^{+/+}$ dams at their respective lengths of pregnancy (p>0.05). **(B)** Measured embryo surface areas of male (left) and female (right) versus embryonic age. The areas of *Naa10*$^{-/Y}$ and *Naa10*$^{+/-}$ embryos are not statistically different from those of wildtype (*Naa10*$^{+/Y}$ and *Naa10*$^{+/+}$) embryos (p>0.05). **(C)** Embryo weights of male (left) and female (right) versus embryonic age were determined by measurement. The weights of *Naa10*$^{-/Y}$ and *Naa10*$^{+/-}$ embryos are not significantly different from those of wildtype embryos (p>0.05). Graphs **B-C** were produced using nonlinear exponential regression modeling.
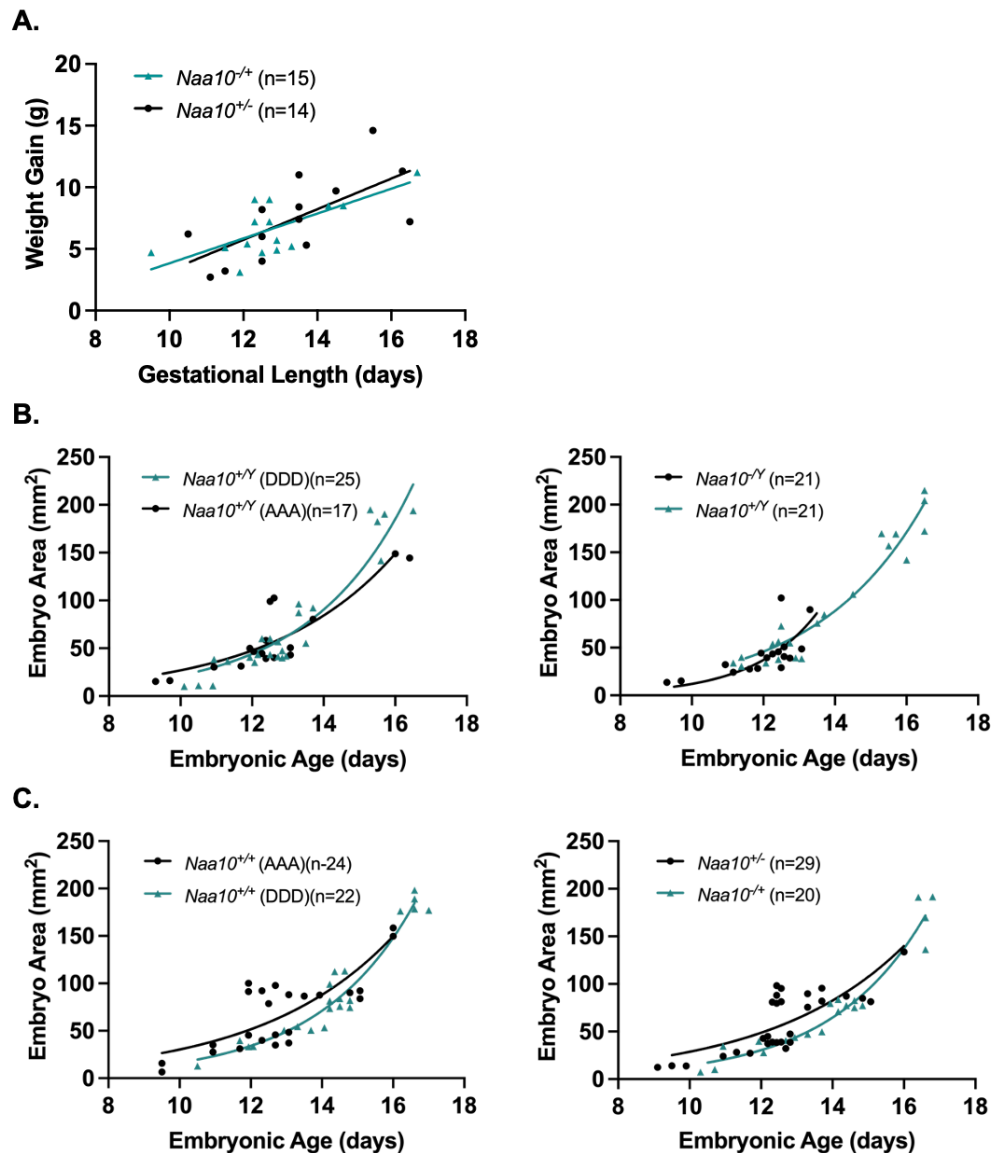
Figure 4. Within-litter analyses for embryos that inherited knockout for *Naa10* maternally and from the maternal grandfather. (A) Male embryo areas age E12.5 are graphed and grouped by litter, which were in cage #6, 7, 8 and 16). Two of the four litters contained more than one *Naa10^{-/Y}* embryo. In all 4 litters, the embryo with the smallest area was the *Naa10^{-/Y}* . **(B)** Male embryo weights age E12.5 are graphed and grouped by litter. 2 out of 4 litters contained more than one *Naa10^{-/Y}* embryo. In 2 out of 4 litters, the embryo with the lowest weight was the *Naa10^{-/Y}*. **(C)** Pictures of E12.5 embryos from litter AAA8: *Naa10^{+/Y}* (1), *Naa10^{-/Y}* (2), *Naa10^{+/+}* (3), *Naa10^{+/-}* (4).

Figure 5. Embryonic phenotypes of *Naa10* knockout mice after 20 backcrosses, maternally inherited but originating from the maternal grandmother, and represented here as DDD. **(A)** *Naa10^-/+* and *Naa10^+/+* dams were weighed and compared at various lengths of gestation. There was no statistically significant difference between both simple linear regression lines that represent the weight gains of *Naa10^+/-* and *Naa10^+/+* dams at their respective length of pregnancy. **(B)** Measured embryo surface areas of male (left) and female (right) versus embryonic age. The areas of *Naa10^-/Y* and *Naa10^-/+* embryos are not significantly different from those of wildtype embryos (p>0.05). **(C)** Embryo weights of male (left) and female (right) versus embryonic age were determined by measurement. The weights of *Naa10^-/Y* and *Naa10^-/+* embryos are not statistically significantly different from those of wildtype (*Naa10^+/Y* and *Naa10^+/+*) embryos (p>0.05). Graphs **B-C** were produced using nonlinear exponential regression modeling.

Figure 6. Within-litter analyses for embryos that inherited knockout for *Naa10* maternally and from the maternal grandmother. **(A)** Male embryo areas age E12.5 are graphed and grouped by litter; two of the three litters contained more than one *Naa10*$^{-/Y}$ embryo. In all three litters, the embryo with the smallest area was the *Naa10*$^{-/Y}$. **(B)** Male embryo weights age E12.5 are graphed and grouped by litter. Two out of three litters contained more than one *Naa10*$^{-/Y}$ embryo. In two out of three litters, the embryo with the lowest weight was the *Naa10*$^{-/Y}$. **(C)** Pictures of E12.5 embryos from litter DDD14: *Naa10*$^{+/Y}$ (1), *Naa10*$^{-/Y}$ (2), *Naa10*$^{+/+}$ (3), *Naa10*$^{-/+}$ (4).
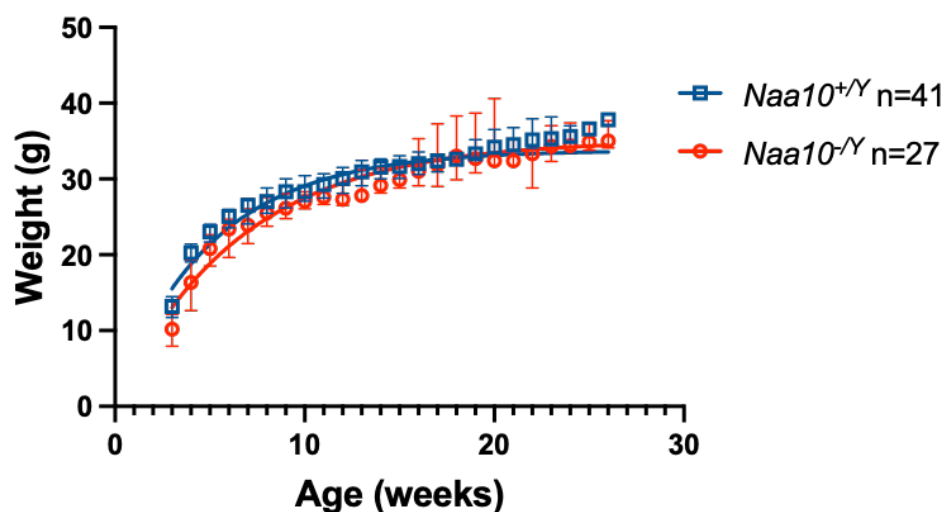
Figure 7. Embryo area versus embryonic age for embryos with maternally inherited *Naa10* knockout allele, where the allele originated from the maternal grandmother (DDD) or the maternal grandfather (AAA). **(A)** Weight gain of *Naa10*$^{-/+}$ (DDD dams) and *Naa10*$^{+/-}$ (AAA dams) at various lengths of gestation were compared. We observed no statistically significant difference between both simple linear regression lines that represent the weight gains of dams from both mating series at each length of pregnancy ($p>0.05$). **(B)** Left: Embryo area versus embryonic age for DDD vs. AAA *Naa10*$^{+/Y}$ males. Right: Embryo area versus embryonic age for DDD vs. AAA *Naa10*$^{-/Y}$ males. **(C)** Left: Embryo area versus embryonic age for DDD vs. AAA *Naa10*$^{+/+}$ females. Right: Embryo area versus embryonic age for DDD *Naa10*$^{-/+}$ vs. AAA *Naa10*$^{+/-}$ females. There are no statistically significant differences between the embryo areas for each genotype from each mouse line ($p>0.05$). Graphs **B-C** were produced using nonlinear exponential regression modeling.

Pleiotropic Effects of *Naa10* Knockout on Postnatal Mice

This current study continues our analysis of the original *Naa10$^{-/Y}$* knockout strain of live born mice, as previously reported (Kweon et al. 2021), but now genetically inbred with more than 20 backcrosses to C57BL/6J (Jackson Laboratories, Bar Harbour, ME). Surviving *Naa10$^{-/Y}$* mice showed decreased body weight when compared to *Naa10$^{+/Y}$* (WT) mice throughout the course of postnatal development. **Figure 8** charts the body weights of male *Naa10$^{-/Y}$* and *Naa10$^{+/Y}$* mice from three to 20 weeks. As displayed in the figure, *Naa10$^{-/Y}$* mice consistently had reduced body weights compared to *Naa10$^{+/Y}$* mice throughout the entire 18-week period where data was collected. The mean body weights of *Naa10$^{-/Y}$* mice presented with lower than the mean body weight when compared to *Naa10$^{+/Y}$* mice. To further assess whether these differences in body weights were significant, *t*-tests were performed comparing the two groups' weight data each week. Analysis shows a statistically significant difference ($p<0.05$) between the weights of *Naa10$^{+/Y}$* and *Naa10$^{-/Y}$* mice in 12 out of 18 weeks. Our observations show that the *Naa10$^{-/Y}$* mice had significantly less body weight than the *Naa10$^{+/Y}$* mice throughout most of their postnatal development with the exception of 6 out of the 18 weeks; specifically in weeks five and 16 through 20. During these six weeks there was no statistically significant difference ($p>0.05$); however, sample sizes were low which may have led to higher variability and lack of significance in these weeks. **Figure 8** shows a phenotypic difference in body weight where the KO mouse is noticeably smaller than the WT littermate mouse. This is similar to the human condition, as some individuals with Ogden syndrome are small in weight and have short stature, whereas a few humans develop at typical size (Sandomirsky et al. 2023).

Other phenotypic defects present in the *Naa10* knockout mice include hydrocephalus, piebaldism, and hydronephrosis (**Table 3**), which are consistent with previous findings (Kweon et al. 2021).

Figure 8. Phenotypic weight data of neonatal $Naa10^{-/Y}$(KO) and $Naa10^{+/Y}$(WT) mice after 20 backcrosses. Male mice body weights were obtained from 3-20 weeks. Twelve out of 18 weeks showed a statistically significant difference in body weights when comparing KO mice to wildtype littermates ($p<0.05$). The graph uses nonlinear exponential regression modeling.

Table 3. Percentage of phenotypes observed in *Naa10$^{-/Y}$* mice vs. C57BL/6J male mice.

Phenotypes	Piebaldism	Hydrocephalus	Hydronephrosis	White digits and tail tips.
Percentage in *Naa10$^{-/Y}$* mice	97% (28/29)	17% (5/29)	27% (3/11)	100% (29/29)
Percentage in male C57BL/6J mice	0%	1.6% (3/191)	Never observed in routine necropsies	0%

Supplementary Figure 12A show an *Naa10$^{-/Y}$* mouse (left) with hydrocephaly as compared to a wildtype littermate with a normally developed skull as well as normal body composition. Hydrocephalus was observed in 17% (5/29) of *Naa10$^{-/Y}$* mice. **Supplementary Figure 12B** displays piebaldism on the ventral abdomen of a *Naa10$^{-/Y}$* mouse, which is a consistent phenotype seen in many *Naa10$^{-/Y}$* mice. This phenotype was observed in 97% (28/29) of *Naa10$^{-/Y}$* mice. The prior paper reported piebaldism in 100% of *Naa10$^{-/Y}$* mice (Kweon et al. 2021). We believe that the one mouse we observed to lack piebaldism may have lost the hypopigmentation during maturation (discussed further below). **Supplementary Figure 12C** displays hydronephrosis in a *Naa10$^{-/Y}$* mouse. The left kidney is noticeably enlarged, with the left kidney weighing 13.02 grams compared to the right kidney weighing 0.34 grams. **Supplementary Figure 12C** also shows that the *Naa10$^{-/Y}$* mouse presenting with hydronephrosis also had an enlarged bladder. The hydronephrosis phenotype was observed in 27% (3/11) of surviving *Naa10$^{-/Y}$* mice.

White digits and tails can be seen in the *Naa10$^{-/Y}$* mice shown in **Supplementary Figures 12A (left)** and **B (left)**, as the *Naa10$^{-/Y}$* mouse exhibits ventral abdominal piebaldism, white tail tips and digits while its wildtype littermate did not. We observed this phenotype in 100% (29/29) of *Naa10* knockout mice on this pure genetic background, displaying its complete penetrance on that background.

Discussion

The impact of genetic background is supported by our observation that additional null alleles (*Naa10* Δ668 and *Naa10* Δ668-674) on mixed genetic backgrounds (~ 75% C57BL/6J, 25% DBA/2J (D2)) have far less penetrance for piebaldism and much less (if any) neonatal lethality, whereas the piebaldism was fully penetrant after eight backcrosses to C57BL/6J for the previously published allele (Kweon et al. 2021), along with the previously reported partial penetrance for ventricular septal defects (VSD), atrial septal defects (ASD), persistent truncus arteriosus (PTA) or double outlet right ventricle (DORV) of the mice who died in the first three days of life (n= 6/28, or 21%) (Kweon et al. 2021). We also previously reported that there was no

embryonic lethality for the *Naa10*$^{-/y}$ mice after eight backcrosses to C57BL/6J, except for when the compensating enzyme Naa12 was knocked out (Kweon et al. 2021). Our study examined this on an inbred C57BL/6J genetic background (20 backcrosses) and in the new environment of the animal facility at IBR, where we did observe some embryonic lethality (~20-25% of *Naa10*$^{-/Y}$ male mice), even in the presence of *Naa12*. It is possible that the pure genetic background (>20 backcrosses with C57BL/6J) is modulating and increasing the severity of the phenotype, thus leading to some embryonic lethality, just as reported in *Pax3* mice (Olaopa et al. 2011). Another possible explanation for embryonic lethality could be that the transfer of all mice to a new animal colony and environment in March 2019 contributed to this embryonic lethality, perhaps by causing maternal stress, as there was a parallel increase in neonatal lethality in the new colony that was observed for all mice, including even the wild type *C57BL/6J* mice (unpublished data). This partially penetrant embryonic lethality phenotype on a pure inbred genetic background in a new animal colony environment occurs despite the presence of the previously reported compensating enzyme, Naa12 (Kweon et al. 2021).

We have previously noted that *Naa10*$^{-/-}$ mutants somewhat phenocopy *Pax3* mutants, as *Pax3*$^{+/-}$ adults have 100% piebaldism, along with variable penetrance for neural crest (NC)-related persistent truncus arteriosus (PTA) or double outlet right ventricle (DORV) with concomitant ventricular septal defects VSDs (Conway, Henderson, and Copp 1997; Conway et al. 1997; van den Hoff and Moorman 2000; Olaopa et al. 2011), congenital hydrocephalus (Zhou and Conway 2016), and/or skeletal defects due to abnormal somite morphogenesis (Henderson, Conway, and Copp 1999; Dickman, Rogers, and Conway 1999). Of most relevance here, the phenotype of *Pax3* nulls can be modulated by genetic background, in which it has been shown that those mice exhibit 100% mid-gestational lethality due to cardiac neural crest-related deficiencies on C57Bl/6J inbred genetic background (Olaopa et al. 2011). As such, there is modulation of these neural crest-related phenotypes by genetic background. There is a long and very extensive literature

regarding the modulation of phenotype by genetic background, some of which is summarized in a book chapter written by one of us (Lyon and O'Rawe 2015, 2014).

A prior study (Lee et al. 2017) found embryonic lethality in mice on a somewhat mixed genetic background, as that strain was used after "at least six generations of backcross with C57BL/6 mice", which was noted by the authors to be the sub-strain C57BL/6JNarl, first established at the Animal Center of National Research Institute from the Jackson Laboratories in 1995. However, as noted, the different environments of the animal facilities may play some role; therefore, embryonic lethality may be somehow more apparent even when the mice are not fully inbred. Also, the previous study (Lee et al. 2017) used the Cre/loxP system to generate the *Naa10* KO mice, where a floxed *Naa10* female mouse was crossed with the Ella-Cre transgenic male mouse expressing Cre recombinase for germ line deletion of loxP-flanked *Naa10*, whereas the Naa10$^{-/y}$ mice were made using standard gene-targeting methods without the use of Cre recombinase (Kweon et al. 2021; Yoon et al. 2014). It is not clear how Cre recombinase could impact the phenotype in the strain maintained at the Taiwan facility. It is notable that the other group did not comment on whether their mice have piebaldism or any skeletal defects, so it is not clear if the mice possess these phenotypes (Lee et al. 2017; Lee et al. 2019).

We report that we cannot replicate the previously reported "maternal effect lethality" and we cannot find any correlation between the sizes of *Naa10*-null embryos and placental weight (Lee et al. 2017). It is possible that additional study of earlier embryonic ages might reveal whether the embryonic lethality starts internally within the embryo or if it is mediated instead by some placental abnormality, as previously claimed (Lee et al. 2017). Since this prior publication, there have been no other publications replicating these effects or the genomic imprinting findings of the paper. There is also still no crystal structure or any other structure showing that *Naa10* has any direct DNA-binding domain or activity. The authors speculated in their paper that the various phenotypes of the mice (growth retardation, embryonic lethality, brain disorder, and maternal-effect lethality) might be caused by a previously unappreciated role for *Naa10* in DNA methylation

and genomic imprinting. Notably , that study was published prior to the discovery of *Naa12* (Kweon et al. 2021), and those results should be re-evaluated in the context of this compensating enzyme. The prior study utilized a small number of mice and samples for the various phenotypes in the mice such as "maternal effect lethality" and were able to only use two embryos of each genotype for the imprinting analyses (Lee et al. 2017). It thus remains an open question in the field whether the various replicated phenotype findings in the mice (such as variable amounts of piebaldism, skeletal defects, small size, hydrocephaly, and hydronephrosis) are due to decreased amino-terminal acetylation of certain key proteins or whether some effect related to DNA methylation or genomic imprinting plays a role. Other groups have published that NAA10 might acetylate lysine side chains as a lysine acetyltransferase (KAT), although this is controversial (Magin, March, and Marmorstein 2016). Future studies are needed to identify acetylated proteins and to study their mechanism of action in both mouse models and humans.

MATERIALS AND METHODS

Experimental animals. All experiments were performed in accordance with guidelines of International Animal Care and Use Committees (IACUC) of Cold Spring Harbor Laboratory (CSHL) and New York State Institute for Basic Research in Developmental Disabilities (IBR). The mice were moved to the IBR facility in March 2019, after being housed at CSHL from 2015-2019. While at CSHL, they were housed as breeding pairs or were weaned and housed by sex in individually ventilated autoclaved caging (Ancare Ventilated Caging, Bellmore, NY). At IBR, animals are maintained in autoclaved cages and bedding with 1/8-inch corn cob bedding (The Andersons, Maumee, OH) and were fed a closed-formula, natural-ingredient, γ-irradiated diet (PicoLab Mouse Diet 5058, Purina LabDiet, St. Louis MO) *ad libitum*, and received tap municipal water in polysulfone bottles (Thoren). Mice receive a sterile supplement Love Mash Rodent Reproductive Diet (Bio-Serv; Flemington, NJ). A complete cage change was performed every 7-10 days within horizontal laminar flow cage change station (model Nu602-400Class II TypeNuaire, Plymouth, MN). The room was maintained on a 10:14-h light: dark cycle with a relative humidity of 30 – 70%, and room temperature ranging from 69-78°F. At IBR, since March 2019, mice were housed in a specific pathogen free room of a conventional animal facility in accordance with the *Guide for the Care and Use of Laboratory Animals* (8th edition)(National Research Council et al. 2011). Mice were housed as breeding pairs or were weaned and housed by sex in individually ventilated autoclaved caging (no. 5, Thoren Caging Systems, Hazelton, PA).

Rodent health monitoring assessment is performed three times a year. Mice in this colony are specific pathogen free for the following; astroviruses types 1 and 2, new world Hantaviruses, lymphocytic choriomeningitis virus, mouse adenovirus types 1 and 2, mouse hepatitis virus, ectromelia virus, mouse kidney parvovirus (murine chapparvovirus), mouse parvovirus, minute

virus of mice, mouse rotavirus (epizootic diarrhea of infant mice virus), pneumonia virus of mice, reovirus, Sendai virus, Theiler meningoencephalitis virus; beta Strep Groups A, B, C and G, *Bordetella bronchiseptica*, *Bordetella pseudohinzii*, *Campylobacter* spp., ciliary-associated respiratory bacillus (*F. rodentium*),*Corynbacterium kutscheri*, *Klebsiella oxytoca*, *Klebsiella pneumoniae*, *Mycoplasma pulmonis*, *Citrobacter rodentium*, *Rodentibacter* spp., *Chlamydia muridarum, Pseudomonas aeruginosa*, *Salmonella* spp., *Streptobacillus moniliformis*, *Proteus mirabilis*, and *Clostridium piliforme*; *Pneumocystis*, *Giardia* spp. and *Spironucleus muris*; and fur mites (*Myobia musculi*, *Myocoptes musculinis*, and *Radfordia affinis*) and pinworms (*Syphacia* spp. and *Aspiculuris* spp.) all of which is based on multiplex polymerase chain reaction pooled from oral swabs, pelt swabs, and fecal pellets obtained directly (representing 10-15% of cages) and serologic panels from a subset (representing ~2% of cages). PCR and serology were performed by Charles River Laboratories (Wilmington, MA).

Generation and genotyping of *Naa10* knockout mice. The *Naa10* knockout (KO) mice were generated as previously described (Yoon, H., et al). The progeny was backcrossed to C57BL/6J for more than 20 generations. This was confirmed with genome scanning at the Jackson Laboratory. The stock of C57BL/6J was replenished annually from Jackson Laboratory (JAX) to avoid genetic drift from the JAX inbred line. Paw tattoo and tail genotyping was performed on day 5 or 6 of life, so as not disturb the litters and thus not increase the risk for maternal rejection of the litter. The primers used for *Naa10 KO* and *Naa10^{tm1a}* genotyping were Naa10-F: 5'-cctcacgtaatgctctgcaa-3', Naa10-neo-F: 5'-acgcgtcaccttaat-atgcg-3', Naa10-R: 5'-tgaaagttgagggtgttgga-3' (**Supplementary Table 8)**.

Generation and genotyping of *Naa10* minigene mice.

Standard methods were used to generate and select ES clones that were used for blastocyst microinjection and generation of chimeric mice. Chimeric mice were mated with C57BL/6 mice,

and germ-line transmission of targeted alleles was detected by PCR. Primers used were: MG1F: 5'-GTCGACGGCTCAGCATGAAGA; Lox1: 5'-AGCTCCTATCGTCCTTTCCCTGC; SQ2: 5'-AACTATGGCCAGCTTGCTATG; and PT4: 5'-TCTCCAGTCTACCTCTACCAAACCC. Ser37Pro Genotyping PCR: MG1F-PT4, 980 bp product; Ser37Pro mutation activation PCR: Lox1-MG1F (730 bp) or Lox1-SQ2 (1150 bp).

Generation of *Naa10* (Gm16286, UniProt: Q9CQX6) indel knockout mice. The mice were made using standard methods by microinjection of CRISPR reagent mix into zygotes obtained from the mating of B6D2F1 females (i.e., 50% C57BL/6J, 50% DBA/2J (D2)) females to inbred C57BL/6J males. The guide RNA was produced and validated from Horizon using a Cel1-nuclease assay, and the most active guide was selected, including the targeting cr-RNA sequence and the tracrRNA portion. The indels were transmitted by breeding again to inbred C57BL/6J males, and the resulting progeny were interbred on a mixed genetic background of approximately 12.5% DBA/2J (D2) / 87.5% C57BL/6J, for use in the reported experiments. Genomic DNA was isolated from paw and tail. DNA was screened for mutations using PCR and Surveyor assay (Qiu et al. 2004), followed by Sanger sequencing of selected clones and the use of CRISP-ID (Dehairs et al. 2016) to identify putative deletions.

Isolation and imaging of mouse embryos. Timed matings were performed by counting the number of days since the male and female were paired. The male mice were left in the cage for three days, prior to removal, giving a three-day window for embryogenesis. Theiler staging was performed for a precise gestational age. Pregnant mice were euthanized at several time points after conception. The embryos were isolated on ice, then washed three times in cold 1% PBS. Embryos were imaged using an Olympus SZX10 with Olympus CellSens imaging software (Center Valley, PA, USA). Both embryos and placentas were measured, weighed, then stored in 10% formalin buffered saline and then stored at four degrees Celsius.

Whole body CT scanning. CT scans were acquired on a Nanoscan PET/CT scanner at CSHL from Mediso using Nucline v2.01 software. All mice were kept sedated under isoflurane anesthesia for the duration of the scan. Scans were acquired with an X-ray tube energy and current of 70kVp and 280uA respectively. 720 projections were acquired per rotation, for 3 rotations, with a scan time of approximately 11 minutes, followed by reconstruction with a RamLak filter and voxel size 40x40x122μm. The relative mean bone density of the femur from these mice was measured in Hounsfield units using VivoQuant software (v2.50patch2). Briefly, the femur was accurately segmented from the image by first applying a ROI about the bone. Global thresholding, with a minimum of 1000 HU and a maximum of 8000 HU was then applied to accurately segment the femur from the initial ROI. For *ex vivo* analyses, mouse heads were fixed in 10% formalin buffered saline, followed by scanning and reconstruction with 1440 projections per revolution. Cranial volume was measured using VivoQuant software (v2.50patch2), using the spline tool to manually draw around the circumference of the cranium on multiple stepwise 2D slices.

Western blot. Adult mice were euthanized in a CO_2 chamber, followed by cervical dislocation. Tissue was dissected and washed in 1% PBS before immediate processing or flash freezing in liquid nitrogen. Fresh or thawed tissue was lysed in RIPA buffer supplemented with protease inhibitor (#R0278, Sigma-Aldrich; #11836170001, Roche) and disrupted using a handheld cordless motorized microtube pestle. Lysate was cleared via centrifugation. Protein quantification was determined via Bradford assay using PrecisionRed Advanced Protein Assay reagent (#ADV01, Cytoskeleton, Denver, CO, USA). Lysate concentration was normalized before dilution in 2X Laemmli Sample buffer with 10% v/v 2-mercaptoethanol. Accordingly, reducing and denaturing SDS-PAGE was conducted on 10% resolving gel (#4561033, Bio-Rad, Hercules, CA, USA) in the Mini-PROTEAN Tetra Cell system. Resolved proteins were transferred to 0.2 μm nitrocellulose membrane (Amersham, Buckinghamshire, UK) using Towbin's transfer buffer (100

V, 30 min). Membranes were dried at least 15 minutes before reactivating in TBS. Reactivated membranes were stained for total protein using REVERT 700 Total Protein stain kit and scanned wet on Odyssey Classic in the 700nm channel (LI-COR, Lincoln, NB, USA). **Supplementary Table 9**.

After scanning, membranes were blocked in 5% non-fat dry milk (1 hr, RT). Blocked membranes were incubated with 1/500 anti-NAA10 Mab (#13357, Cell Signaling Technology, Danvas, MA, USA) diluted in blocking buffer supplemented with 0.1% Tween-20 (overnight, 4°C). After primary incubation, membranes were placed in TBS-T for 5 minutes (3 repetitions). Membranes were then incubated in 1/20,000 goat-anti-rabbit IR800 CW secondary antibody diluted in blocking buffer (1 hr, RT). Stained membranes were washed in TBS-T for 5 minutes (3 repetitions) and rinsed in TBS. Membranes were dried before scanning on the Odyssey Classic. NAA10 signal was normalized to total protein as indicated by REVERT 700 stains; normalized NAA10 signal was quantified in Empiria Studio (LI-COR). Hypothesis testing was conducted in RStudio. Western blot datasets and analyses are available on Github (https://github.com/ajgarcuny).

Measurement of Piebaldism

While at CSHL, photographs of anesthetized or euthanized mice with piebaldism were obtainedusing a digital camera with a ruler alongside each animal to facilitate measurement of the surface area of the spotting, using the software program ImageJ (National Institute of Health, Public Domain, BSD-2). For those mice photographed during anesthesia, they were continually sedated with isoflurane, and many of these mice underwent CT scanning. Mice were weighed at the time of photography. Data were plotted using GraphPad Prism (New York, NY, USA) 6 for Macintosh IOS.

Data Analysis

Prism 9 Graphpad software version 9.5.1(528) (San Diego, CA, USA) and Microsoft Excel version 16.72 (Redmond, WA, USA) were used.

REFERENCES

Afrin, Antara, Jeremy W. Prokop, Adam Underwood, Katie L. Uhl, Elizabeth A. VanSickle, Roja Baruwal, Morgan Wajda, Surender Rajasekaran, and Caleb Bupp. 2020. "NAA10 Variant in 38-Week-Gestation Male Patient: A Case Study." *Cold Spring Harbor Molecular Case Studies* 6 (6). https://doi.org/10.1101/mcs.a005868.

Aksnes, Henriette, Rasmus Ree, and Thomas Arnesen. 2019. "Co-Translational, Post-Translational, and Non-Catalytic Roles of N-Terminal Acetyltransferases." *Molecular Cell* 73 (6): 1097–1114.

Arnesen, T., M. J. Betts, F. Pendino, D. A. Liberles, D. Anderson, J. Caro, X. Kong, J. E. Varhaug, and J. R. Lillehaug. 2006. "Characterization of HARD2, a Processed HARD1 Gene Duplicate, Encoding a Human Protein N-Alpha-Acetyltransferase." *BMC Biochemistry* 7: 13.

Arnesen, Thomas, Dave Anderson, Christian Baldersheim, Michel Lanotte, Jan E. Varhaug, and Johan R. Lillehaug. 2005. "Identification and Characterization of the Human ARD1-NATH Protein Acetyltransferase Complex." *The Biochemical Journal* 386 (Pt 3): 433–43.

Arnesen, Thomas, Kristian K. Starheim, Petra Van Damme, Rune Evjenth, Huyen Dinh, Matthew J. Betts, Anita Ryningen, Joël Vandekerckhove, Kris Gevaert, and Dave Anderson. 2010. "The Chaperone-like Protein HYPK Acts Together with NatA in Cotranslational N-Terminal Acetylation and Prevention of Huntingtin Aggregation." *Molecular and Cellular Biology* 30 (8): 1898–1909.

Arnesen, Thomas, Petra Van Damme, Bogdan Polevoda, Kenny Helsens, Rune Evjenth, Niklaas Colaert, Jan Erik Varhaug, et al. 2009. "Proteomics Analyses Reveal the Evolutionary Conservation and Divergence of N-Terminal Acetyltransferases from Yeast and Humans." *Proceedings of the National Academy of Sciences of the United States of America* 106 (20): 8157–62.

Bader, Ingrid, Nina McTiernan, Christine Darbakk, Eugen Boltshauser, Rasmus Ree, Sabine Ebner, Johannes A. Mayr, and Thomas Arnesen. 2020. "Severe Syndromic ID and Skewed X-Inactivation in a Girl with NAA10 Dysfunction and a Novel Heterozygous de Novo NAA10 p.(His16Pro) Variant - a Case Report." *BMC Medical Genetics* 21 (1): 153.

Blomen, Vincent A., Peter Májek, Lucas T. Jae, Johannes W. Bigenzahn, Joppe Nieuwenhuis, Jacqueline Staring, Roberto Sacco, et al. 2015. "Gene Essentiality and Synthetic Lethality in Haploid Human Cells." *Science (New York, N.Y.)* 350 (6264): 1092–96.

Casey, Jillian P., Svein I. Støve, Catherine McGorrian, Joseph Galvin, Marina Blenski, Aimee Dunne, Sean Ennis, et al. 2015. "NAA10 Mutation Causing a Novel Intellectual Disability Syndrome with Long QT Due to N-Terminal Acetyltransferase Impairment." *Scientific Reports* 5 (November): 16022.

Chen, Di, Jiuli Zhang, Justin Minnerly, Tiffany Kaul, Donald L. Riddle, and Kailiang Jia. 2014. "Daf-31 Encodes the Catalytic Subunit of N Alpha-Acetyltransferase That Regulates Caenorhabditis Elegans Development, Metabolism and Adult Lifespan." *PLoS Genetics* 10 (10): e1004699.

Chen, Hongyu, Shuqin Li, Lu Li, Weiying Wu, Xiaolong Ke, Wenxuan Zou, and Jie Zhao. 2018. "Nα-Acetyltransferase 10 and 15 Are Required for the Correct Initiation of Endosperm Cellularization in Arabidopsis." *Plant & Cell Physiology* 59 (10): 2113–28.

Cheng, H., A. V. Dharmadhikari, S. Varland, N. Ma, D. Domingo, R. Kleyner, A. F. Rope, et al. 2018. "Truncating Variants in NAA15 Are Associated with Variable Levels of Intellectual Disability, Autism Spectrum Disorder, and Congenital Anomalies." *American Journal of Human Genetics* 102 (5): 985–94.

Cheng, Hanyin, Leah Gottlieb, Elaine Marchi, Robert Kleyner, Puja Bhardwaj, Alan F. Rope, Sarah Rosenheck, et al. 2019. "Phenotypic and Biochemical Analysis of an International Cohort of Individuals with Variants in NAA10 and NAA15." *Human Molecular Genetics*, May. https://doi.org/10.1093/hmg/ddz111.

Conway, S. J., D. J. Henderson, and A. J. Copp. 1997. "Pax3 Is Required for Cardiac Neural Crest Migration in the Mouse: Evidence from the Splotch (Sp2H) Mutant." *Development* 124 (2): 505–14.

Conway, S. J., D. J. Henderson, M. L. Kirby, R. H. Anderson, and A. J. Copp. 1997.

"Development of a Lethal Congenital Heart Defect in the Splotch (Pax3) Mutant Mouse."

Cardiovascular Research 36 (2): 163–73.

Dehairs, Jonas, Ali Talebi, Yacine Cherifi, and Johannes V. Swinnen. 2016. "CRISP-ID:

Decoding CRISPR Mediated Indels by Sanger Sequencing." *Scientific Reports* 6 (1).

https://doi.org/10.1038/srep28973.

Dickman, E. D., R. Rogers, and S. J. Conway. 1999. "Abnormal Skeletogenesis Occurs

Coincident with Increased Apoptosis in the Splotch (Sp2H) Mutant: Putative Roles for

Pax3 and PDGFRalpha in Rib Patterning." *The Anatomical Record* 255 (3): 353–61.

Dikiy, Igor, and David Eliezer. 2014. "N-Terminal Acetylation Stabilizes N-Terminal Helicity in

Lipid- and Micelle-Bound α-Synuclein and Increases Its Affinity for Physiological

Membranes." *The Journal of Biological Chemistry* 289 (6): 3652–65.

Dörfel, M. J., and G. J. Lyon. 2015. "The Biological Functions of Naa10 - from Amino-Terminal

Acetylation to Human Disease." *Gene* 567 (2): 103–31.

Dörfel, Max J., Han Fang, Jonathan Crain, Michael Klingener, Jake Weiser, and Gholson J.

Lyon. 2017. "Proteomic and Genomic Characterization of a Yeast Model for Ogden

Syndrome." *Yeast* 34 (1): 19–37.

Esmailpour, Taraneh, Hamidreza Riazifar, Linan Liu, Sandra Donkervoort, Vincent H. Huang,

Shreshtha Madaan, Bassem M. Shoucri, et al. 2014. "A Splice Donor Mutation in NAA10

Results in the Dysregulation of the Retinoic Acid Signalling Pathway and Causes Lenz

Microphthalmia Syndrome." *Journal of Medical Genetics* 51 (3): 185–96.

Feng, Jinlin, Ruiqi Li, Junya Yu, Shuangshuang Ma, Chunyan Wu, Yan Li, Ying Cao, and

Ligeng Ma. 2016. "Protein N-Terminal Acetylation Is Required for Embryogenesis in

Arabidopsis." *Journal of Experimental Botany* 67 (15): 4779–89.

Gogoll, Laura, Katharina Steindl, Pascal Joset, Markus Zweier, Alessandra Baumer, Christina

Gerth-Kahlert, Boris Tutschek, and Anita Rauch. 2021. "Confirmation of Ogden

Syndrome as an X-Linked Recessive Fatal Disorder Due to a Recurrent NAA10 Variant and Review of the Literature." *American Journal of Medical Genetics. Part A* 185 (8): 2546–60.

Gottlieb, Leah, and Ronen Marmorstein. 2018. "Structure of Human NatA and Its Regulation by the Huntingtin Interacting Protein HYPK." *Structure* 26 (7): 925-935.e8.

Gupta, Angela S., Hind Al Saif, Jennifer M. Lent, and Natario L. Couser. 2019. "Ocular Manifestations of the NAA10-Related Syndrome." *Case Reports in Genetics* 2019 (April): 8492965.

Henderson, D. J., S. J. Conway, and A. J. Copp. 1999. "Rib Truncations and Fusions in the Sp2H Mouse Reveal a Role for Pax3 in Specification of the Ventro-Lateral and Posterior Parts of the Somite." *Developmental Biology* 209 (1): 143–58.

Hoff, M. J. van den, and A. F. Moorman. 2000. "Cardiac Neural Crest: The Holy Grail of Cardiac Abnormalities?" *Cardiovascular Research* 47 (2): 212–16.

Hofman, Jagoda, Michal Hutny, Karolina Chwialkowska, Urszula Korotko, Karolina Loranc, Anna Kruk, Urszula Lechowicz, et al. 2022. "Case Report: Rare among Ultrarare-Clinical Odyssey of a New Patient with Ogden Syndrome." *Frontiers in Genetics* 13 (September): 979377.

Holmes, William M., Brian K. Mannakee, Ryan N. Gutenkunst, and Tricia R. Serio. 2014. "Loss of Amino-Terminal Acetylation Suppresses a Prion Phenotype by Modulating Global Protein Folding." *Nature Communications* 5 (July): 4383.

Johnston, Jennifer J., Kathleen A. Williamson, Christopher M. Chou, Julie C. Sapp, Morad Ansari, Heather M. Chapman, David N. Cooper, et al. 2019. "NAA10 Polyadenylation Signal Variants Cause Syndromic Microphthalmia." *Journal of Medical Genetics*, March, jmedgenet-2018.

Kweon, Hyae Yon, Mi-Ni Lee, Max Dorfel, Seungwoon Seo, Leah Gottlieb, Thomas PaPazyan, Nina McTiernan, et al. 2021. "Naa12 Compensates for Naa10 in Mice in the Amino-Terminal Acetylation Pathway." *ELife* 10 (August). https://doi.org/10.7554/eLife.65952.

Lee, C. C., S. H. Peng, L. Shen, C. F. Lee, T. H. Du, M. L. Kang, G. L. Xu, et al. 2017. "The Role of N-Alpha-Acetyltransferase 10 Protein in DNA Methylation and Genomic Imprinting." *Molecular Cell*. https://doi.org/10.1016/j.molcel.2017.08.025.

Lee, Chen-Cheng, Yi-Chun Shih, Ming-Lun Kang, Yi-Cheng Chang, Lee-Ming Chuang, Ramanan Devaraj, and Li-Jung Juan. 2019. "Naa10p Inhibits Beige Adipocyte-Mediated Thermogenesis through N-α-Acetylation of Pgc1α." *Molecular Cell* 76 (3): 500-515.e8.

Linster, Eric, Iwona Stephan, Willy V. Bienvenut, Jodi Maple-Grødem, Line M. Myklebust, Monika Huber, Michael Reichelt, et al. 2015. "Downregulation of N-Terminal Acetylation Triggers ABA-Mediated Drought Responses in Arabidopsis." *Nature Communications* 6 (1): 7640.

Lyon, G. J. 2011. "Personal Account of the Discovery of a New Disease Using Next-Generation Sequencing. Interview by Natalie Harrison." *Pharmacogenomics* 12 (11): 1519–23.

Lyon, Gholson J., and Jason O'Rawe. 2014. "Human Genetics and Clinical Aspects of Neurodevelopmental Disorders." *BioRxiv*. https://doi.org/10.1101/000687.

———. 2015. "Human Genetics and Clinical Aspects of Neurodevelopmental Disorders." In *The Genetics of Neurodevelopmental Disorders.*, edited by Kevin Mitchell. Wiley).

Lyon, Gholson J., Marall Vedaie, Travis Besheim, Agnes Park, Elaine Marchi, Leah Gottlieb, Katherine Sandomirsky, et al. 2022. "Expanding the Phenotypic Spectrum of Ogden Syndrome (NAA10-Related Neurodevelopmental Syndrome) and NAA15-Related Neurodevelopmental Syndrome." *MedRxiv*. https://doi.org/10.1101/2022.08.22.22279061.

Magin, R. S., Z. M. March, and R. Marmorstein. 2016. "The N-Terminal Acetyltransferase Naa10/ARD1 Does Not Acetylate Lysine Residues." *The Journal of Biological Chemistry*. https://doi.org/10.1074/jbc.M115.709428.

Maini, Ilenia, Stefano G. Caraffi, Francesca Peluso, Lara Valeri, Davide Nicoli, Steven Laurie, Chiara Baldo, Orsetta Zuffardi, and Livia Garavelli. 2021. "Clinical Manifestations in a Girl with NAA10-Related Syndrome and Genotype–Phenotype Correlation in Females." *Genes* 12 (6): 900.

McTiernan, Nina, Harinder Gill, Carlos E. Prada, Harry Pachajoa, Juliana Lores, CAUSES study, and Thomas Arnesen. 2021. "NAA10 p.(N101K) Disrupts N-Terminal Acetyltransferase Complex NatA and Is Associated with Developmental Delay and Hemihypertrophy." *European Journal of Human Genetics: EJHG* 29 (2): 280–88.

McTiernan, Nina, Lisbeth Tranebjærg, Anna S. Bjørheim, Jacob S. Hogue, William G. Wilson, Berkley Schmidt, Melissa M. Boerrigter, et al. 2022. "Biochemical Analysis of Novel NAA10 Variants Suggests Distinct Pathogenic Mechanisms Involving Impaired Protein N-Terminal Acetylation." *Human Genetics*, January. https://doi.org/10.1007/s00439-021-02427-4.

Mullen, J. R., P. S. Kayne, R. P. Moerschell, S. Tsunasawa, M. Gribskov, M. Colavito-Shepanski, M. Grunstein, F. Sherman, and R. Sternglanz. 1989. "Identification and Characterization of Genes and Mutants for an N-Terminal Acetyltransferase from Yeast." *The EMBO Journal* 8 (7): 2067–75.

Myklebust, L. M., P. Van Damme, S. I. Stove, M. J. Dörfel, A. Abboud, T. V. Kalvik, C. Grauffel, et al. 2015. "Biochemical and Cellular Analysis of Ogden Syndrome Reveals Downstream Nt-Acetylation Defects." *Human Molecular Genetics* 24 (7): 1956–76.

National Research Council, Division on Earth and Life Studies, Institute for Laboratory Animal Research, and Committee for the Update of the Guide for the Care and Use of

Laboratory Animals. 2011. *Guide for the Care and Use of Laboratory Animals: Eighth Edition*. National Academies Press.

Olaopa, M., H. M. Zhou, P. Snider, J. Wang, R. J. Schwartz, A. M. Moon, and S. J. Conway. 2011. "Pax3 Is Essential for Normal Cardiac Neural Crest Morphogenesis but Is Not Required during Migration nor Outflow Tract Septation." *Developmental Biology* 356 (2): 308–22.

Pang, A. L., J. Clark, W. Y. Chan, and O. M. Rennert. 2011. "Expression of Human NAA11 (ARD1B) Gene Is Tissue-Specific and Is Regulated by DNA Methylation." *Epigenetics: Official Journal of the DNA Methylation Society* 6 (11): 1391–99.

Polevoda, B., T. Arnesen, and F. Sherman. 2009. "A Synopsis of Eukaryotic Nalpha-Terminal Acetyltransferases: Nomenclature, Subunits and Substrates." *BMC Proceedings* 3 Suppl 6: S2.

Polevoda, Bogdan, and Fred Sherman. 2003. "Composition and Function of the Eukaryotic N-Terminal Acetyltransferase Subunits." *Biochemical and Biophysical Research Communications* 308 (1): 1–11.

Popp, B., S. I. Stove, S. Endele, L. M. Myklebust, J. Hoyer, H. Sticht, S. Azzarello-Burri, A. Rauch, T. Arnesen, and A. Reis. 2015. "De Novo Missense Mutations in the NAA10 Gene Cause Severe Non-Syndromic Developmental Delay in Males and Females." *European Journal of Human Genetics: EJHG* 23 (5): 602–9.

Qiu, Peter, Harini Shandilya, James M. D'Alessio, Kevin O'Connor, Jeffrey Durocher, and Gary F. Gerard. 2004. "Mutation Detection Using Surveyor Nuclease." *BioTechniques* 36 (4): 702–7.

Ree, R., S. Varland, and T. Arnesen. 2018. "Spotlight on Protein N-Terminal Acetylation." *Experimental & Molecular Medicine* 50 (7): 90.

Ree, Rasmus, Anni Sofie Geithus, Pernille Mathiesen Tørring, Kristina Pilekær Sørensen, Mads Damkjær, DDD study, Sally Ann Lynch, and Thomas Arnesen. 2019. "A Novel NAA10

p.(R83H) Variant with Impaired Acetyltransferase Activity Identified in Two Boys with ID and Microcephaly." *BMC Medical Genetics* 20 (1): 101.

Ritter, Alyssa, Justin H. Berger, Matthew Deardorff, Kosuke Izumi, Kimberly Y. Lin, Livija Medne, and Rebecca C. Ahrens-Nicklas. 2021. "Variants in NAA15 Cause Pediatric Hypertrophic Cardiomyopathy." *American Journal of Medical Genetics. Part A* 185 (1): 228–33.

Rope, A. F., K. Wang, R. Evjenth, J. Xing, J. J. Johnston, J. J. Swensen, W. E. Johnson, et al. 2011. "Using VAAST to Identify an X-Linked Disorder Resulting in Lethality in Male Infants Due to N-Terminal Acetyltransferase Deficiency." *American Journal of Human Genetics* 89 (1): 28–43.

Sandomirsky, Katherine, Elaine Marchi, Maureen Gavin, Karen Amble, and Gholson J. Lyon. 2023. "Phenotypic Variability and Gastrointestinal Manifestations/Interventions for Growth in NAA10-Related Neurodevelopmental Syndrome." *American Journal of Medical Genetics. Part A*, February. https://doi.org/10.1002/ajmg.a.63152.

Saunier, C., S. I. Stove, B. Popp, B. Gerard, M. Blenski, N. AhMew, C. de Bie, et al. 2016. "Expanding the Phenotype Associated with NAA10-Related N-Terminal Acetylation Deficiency." *Human Mutation* 37 (8): 755–64.

Scott, D. C., J. K. Monda, E. J. Bennett, J. W. Harper, and B. A. Schulman. 2011. "N-Terminal Acetylation Acts as an Avidity Enhancer within an Interconnected Multiprotein Complex." *Science* 334 (6056): 674–78.

Shemorry, Anna, Cheol-Sang Hwang, and Alexander Varshavsky. 2013. "Control of Protein Quality and Stoichiometries by N-Terminal Acetylation and the N-End Rule Pathway." *Molecular Cell* 50 (4): 540–51.

Starheim, K. K., K. Gevaert, and T. Arnesen. 2012. "Protein N-Terminal Acetyltransferases: When the Start Matters." *Trends in Biochemical Sciences* 37 (4): 152–61.

Støve, Svein Isungset, Marina Blenski, Asbjørg Stray-Pedersen, Klaas J. Wierenga, Shalini N. Jhangiani, Zeynep Coban Akdemir, David Crawford, et al. 2018. "A Novel NAA10 Variant with Impaired Acetyltransferase Activity Causes Developmental Delay, Intellectual Disability, and Hypertrophic Cardiomyopathy." *European Journal of Human Genetics: EJHG* 26 (9): 1294–1305.

Tian, Yu, Hua Xie, Shenghai Yang, Shaofang Shangguan, Jianhong Wang, Chunhua Jin, Yu Zhang, et al. 2022. "Possible Catch-Up Developmental Trajectories for Children with Mild Developmental Delay Caused by NAA15 Pathogenic Variants." *Genes* 13 (3). https://doi.org/10.3390/genes13030536.

Van Damme, Petra, Svein I. Støve, Nina Glomnes, Kris Gevaert, and Thomas Arnesen. 2014. "A Saccharomyces Cerevisiae Model Reveals in Vivo Functional Impairment of the Ogden Syndrome N-Terminal Acetyltransferase NAA10 Ser37Pro Mutant." *Molecular & Cellular Proteomics: MCP* 13 (8): 2031–41.

Wang, Tim, Kıvanç Birsoy, Nicholas W. Hughes, Kevin M. Krupczak, Yorick Post, Jenny J. Wei, Eric S. Lander, and David M. Sabatini. 2015. "Identification and Characterization of Essential Genes in the Human Genome." *Science (New York, N.Y.)* 350 (6264): 1096–1101.

Wang, Ying, Michelle Mijares, Megan D. Gall, Tolga Turan, Anna Javier, Douglas J. Bornemann, Kevin Manage, and Rahul Warrior. 2011. "Drosophila Variable Nurse Cells Encodes Arrest Defective 1 (ARD1), the Catalytic Subunit of the Major N-Terminal Acetyltransferase Complex." *Developmental Dynamics: An Official Publication of the American Association of Anatomists* 240 (2): spcone-spcone.

Ward, Tarsha, Warren Tai, Sarah Morton, Francis Impens, Petra Van Damme, Delphi Van Haver, Evy Timmerman, et al. 2021. "Mechanisms of Congenital Heart Disease Caused by NAA15 Haploinsufficiency." *Circulation Research* 128 (8): 1156–69.

Yoon, H., H. L. Kim, Y. S. Chun, D. H. Shin, K. H. Lee, C. S. Shin, D. Y. Lee, et al. 2014.

"NAA10 Controls Osteoblast Differentiation and Bone Formation as a Feedback

Regulator of Runx2." *Nature Communications* 5: 5176.

Zhou, H. M., and S. J. Conway. 2016. "Restricted Pax3 Deletion within the Neural Tube Results

in Congenital Hydrocephalus." *J Dev Biol* 4 (1). https://doi.org/10.3390/jdb4010007.